Associated conference: 5th International Small Sample Test Techniques Conference

Conference location: Swansea University, Bay Campus

Conference date: 10th - 12 July 2018

How to cite: Chica, J.C. Díez, P.M.B., Calzada, M.P. 2018. Development of an improved correlation method for the yield strength of steel alloys in the small punch test. *Ubiquity Proceedings*, 1(S1): 12 DOI: https://doi.org/10.5334/uproc.12

Published on: 10 September 2018

UBIQUITY PROCEEDINGS

ubiquity press open access https://ubiquityproceedings.com

Development of an improved correlation method for the yield strength of steel alloys in the small punch test

J. Calaf Chica [1]*, P.M. Bravo Díez [2] and M. Preciado Calzada [3]

[1] Universidad de Burgos; jcalaf@ubu.es
[2] Universidad de Burgos; pmbravo@ubu.es
[3] Universidad de Burgos; mpreciado@ubu.es
***** Correspondence: jcalaf@ubu.es; Tel.: +34-660040883

Abstract: The Small Punch Test (SPT) is a miniaturized test to characterize the mechanical properties of the materials. The load-displacement curve obtained by this test does not directly provide the material parameters, and linear correlations between data obtained from SPT curve and each mechanical property are necessary. The main difficulty of these correlation methods is the high level of scattering showed when analyzing a wide set of materials in the same study. In this paper, a finite element analysis focused on steel alloys was performed to understand the specimen behavior in the early stages of the SPT. Present methods to correlate the material yield strength with the data obtained from the SPT curve were also analyzed via this FEM study to discover the meaning of the current correlation scattering for this mechanical property. This numerical research also proved the accuracy of the proposed correlation method for the yield strength via the SPT. The maximum slope of zone I (Slopeini) of the SPT curve showed an accurate correlation with this mechanical property. Focusing on steel alloys, experimental tensile tests and SPT's were performed to validate the numerical analysis and to demonstrate the suitability of the proposed Slopeini versus yield strength correlation method.

Keywords: Small Punch Test; SPT; yield strength.

1. Introduction

In the early 1980s an innovative Miniaturized Disk Bend Test (MDBT) was developed as a cost-effective method to test the post-irradiated state of materials used in thermonuclear reactor applications [1-2]. Many researchers have investigated and improved this test, developing the Small Punch Test (SPT) as a test method for characterization. It consists of a punch which deforms a firmly gripped specimen between two dies until fracture (see Fig. 1(a)). Research and investigation in the SPT were focused on the evaluation of material properties, including the elastic modulus, yield strength and tensile strength [3-5], ductile-brittle transition [6], fracture properties [7-10], etc. The significant interest shown by researchers in this testing procedure motivated the development of a CEN Code of Practice for the application and use of the small punch test method for metallic materials [11].

Results data recorded during SPT are the load/displacement curves (see Fig. 1(b)). Zones distinguished in this curve are [12]:

Zone I: elastic bending.
Zone II: transition between elastic and plastic bending.
Zone III: plastic hardening.
Zone IV: softening due to material damage initiation.
Zone V: crack growth with a circular shape around the center of the specimen until failure.

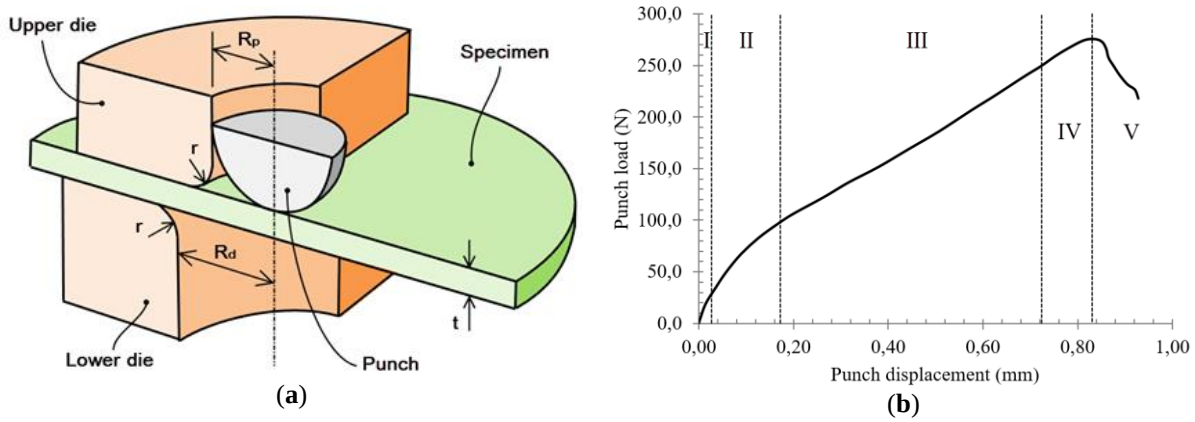

Figure 1. (**a**) Small Punch Test geometry; (**b**) Main behavior zones in the SPT curve.

Nowadays, there are four different methods to obtain the yield strength from the SPT curve:

a. Mao's method [7]. Also referred to as the "two tangents" method, the yield load P_y is obtained from the intersection between two lines: a tangent to the elastic zone I of the SPT curve and another tangent to the plastic zone III of the SPT curve. Both zones I and III do not show any linear behavior so, the tangent to zone I is calculated for the point with the maximum slope, and the tangent to zone III for the point with the minimum slope.
b. Modified Mao's method [13]. The point obtained from the previous "two tangents" method is projected vertically to the SPT curve to obtain the yield load P_y.
c. t/10 method [14]. The yield load P_y is obtained in a way that is similar to σ_y (offset: 0.2%) in standard tensile tests. A parallel line with the tangent to the elastic zone I of the SPT curve is drawn with an offset equal to t/10 in the displacement axis. The intersection of this line with the SPT curve is identified as the yield load P_y.
d. CWA method [11]. Also referred as the "two secants" method, it is like the "two tangents" or Mao method, except for the use of secants instead of tangents. Yield load P_y is calculated by the intersection of two linear functions (two secants), which are calculated minimizing the error between these functions and the SPT curve. CWA [11] recommends the vertical projection of this intersection point to the SPT curve to obtain the most reliable P_y value via this method.

In the early days of SPT research, the SPT curve was performed with the displacement measured using an extensometer installed between upper and lower arms of the assembly (hereinafter referred to as δ_{ext}). Later, an LVDT (Linear Variable Differential Transformer) sensor installed in contact with the lower face of the specimen was used to obtain the displacement data (hereinafter referred to as δ_{lower}). The main differences between these two displacements are:

a. The plastic indentation between the punch and the upper face of the specimen in the initial stages of the zone I of the SPT curve is suppressed in δlower. Thus, zone I becomes a pure elastic region.
b. Non-linear contact deformations between all parts involved in the punch configuration influence the displacement measurement δext.

Point (b) is solved with a correction in the extensometer measurement. The lower die of the SPT is substituted by a tungsten cylinder with an outer diameter and height equal to the lower die dimensions. After a first loading step to a maximum load, which should not be surpassed in the subsequent SPTs, some unloading-loading cycles are performed until the stabilization in the load-displacement δ_{ext} curve is reached. The last loading step of this calibration test is recorded, and a 5th order polynomial regression from this data is established as a calibration function. This curve is used to correct the δ_{ext} obtained from the SPT tests, and it results in a new displacement δ_{upper} equal to the displacement of the upper face of the specimen.

Point (a) is considered by some researchers as the main reason to consider δ_{lower} as more reliable data than δ_{upper} to measure the displacement for the SPT curve [13]. The non-linear behavior of the initial stages of zone I of the SPT curve when δ_{upper} is used is the main reason to discard this method.

2. Materials and Methods

In this article, a first investigation is focused on FEM analyses to:

a. Demonstrate that the accuracy of the correlation obtained from both displacements (δ_{upper} and δ_{lower}) is similar.
b. Perform a detailed analysis of the dependency of the yield load P_y of the SPT curve with more than one plastic property to demonstrate the arbitrary character of the current P_y - σ_y correlations.
c. Validate numerically an alternative method for obtaining the yield strength σ_y with the SPT which shows a high level of dependency on the yield strength of the material and no significant alterations with the rest of the plastic properties.

Finally, as a second part of this investigation, experimental tests (uniaxial tensile tests and SPTs) were performed to demonstrate the suitability of the previous numerical study.

FEM simulations were performed with Abaqus FE software, taking into consideration 36 hypothetical materials. The plastic behavior for all materials was simulated with an isotropic hardening model following the Ramberg-Osgood equation (see Equations 1 and 2 [15]):

$$\varepsilon = \frac{\sigma}{E} + \varepsilon_{offset}\left(\frac{\sigma}{\sigma_y}\right)^n \tag{1}$$

$$n = \frac{\ln\left(\frac{\varepsilon_m - \sigma_m/E}{\varepsilon_{offset}}\right)}{\ln\left(\frac{\sigma_m}{\sigma_y}\right)} \tag{2}$$

where ε_{offset} = 0.002 is the offset strain used to calculate the yield strength.

The elastic properties of all these materials were fixed to E = 200000 MPa and υ = 0.3, and plastic properties were selected to have nine families (M1.y to M9.y) with different yield strengths (100, 250, 400, 550, 700, 850, 1000, 1200 and 1400 MPa). Each of these families had four different Ramberg-Osgood coefficients n (6.95, 8.95, 14 and 35). Table 1 shows the plastic properties assigned for each hypothetical material.

Table 1. Plastic properties of the hypothetical materials

Material	σ_y (MPa)	n*	Material	σ_y (MPa)	n*
M1.1	100	6.95	M5.3	700	14
M1.2	100	8.95	M5.4	700	35
M1.3	100	14	M6.1	850	6.95
M1.4	100	35	M6.2	850	8.95
M2.1	250	6.95	M6.3	850	14
M2.2	250	8.95	M6.4	850	35
M2.3	250	14	M7.1	1000	6.95
M2.4	250	35	M7.2	1000	8.95
M3.1	400	6.95	M7.3	1000	14
M3.2	400	8.95	M7.4	1000	35
M3.3	400	14	M8.1	1200	6.95
M3.4	400	35	M8.2	1200	8.95
M4.1	550	6.95	M8.3	1200	14
M4.2	550	8.95	M8.4	1200	35
M4.3	550	14	M9.1	1400	6.95
M4.4	550	35	M9.2	1400	8.95
M5.1	700	6.95	M9.3	1400	14
M5.2	700	8.95	M9.4	1400	35

Material	σ_y (MPa)	n*	Material	σ_y (MPa)	n*

(*) Hardening coefficient of equations (1) and (2)

In FEM simulations, the specimen thickness was set at 0.5 mm. The rest of the geometric parameters were: R_d=2.0 mm, R_p=1.25 mm and r=0.5 mm (see Fig. 1).

In the experimental tests, six different steels were selected to obtain a wide range of yield strengths from 160 MPa to 1215 MPa. Table 2 shows the mechanical properties of these materials.

Table 2. Mechanical properties of the experimental materials

Material	E (MPa)	σ_y (MPa)	σ_{u_eng} (MPa)	ε_{fract} (mm/mm)
DC04 (1.0338)	203000	160	288.00	0.47
HC300LA (1.0489)	206000	322	411.00	0.31
DC01 (1.0330)	208000	229	353.00	0.35
F1110 (1.0401)	216430	550.60	615.60	0.19
F1140 (1.1191)	204910	745.00	922.67	0.10
15-5PH H900 (1.4545)	194926	1215.00	1310.00	0.16

3. Results

3.1. Numerical analyses

Abaqus was the software selected to perform the numerical analyses for this research. SPT simulation was done with an implicit method in an axisymmetric model (see Fig. 2). The specimen was meshed with quadrilateral elements with reduced integration and hourglass control (CAX4R) and with a global size of 0.025 mm per cell. The spherical punch and upper and lower dies were simulated as analytical rigid bodies. Interaction between each part was simulated with the standard surface-to-surface contact algorithm with a friction coefficient of μ = 0.18 (typical value for steel-steel contact). Elastic and plastic material properties used for each analysis are shown in Table 1.

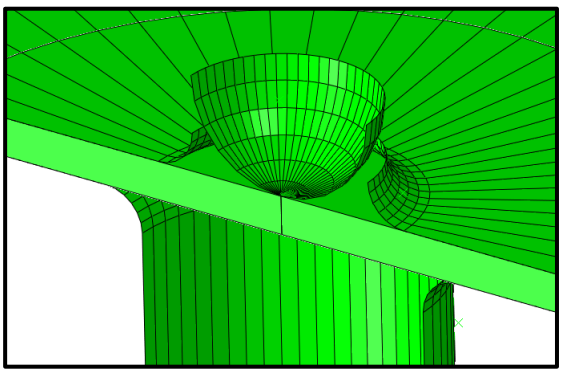

Figure 2. SPT FE model.

Thirty-six hypothetical materials M1.1 to M9.4 (see Table 1 for the mechanical properties of these materials) were simulated with the same FE model used in the previous section. Fig. 3 represents the load-displacement SPT curves for four hypothetical materials M1.1 to M1.4. Two types of SPT curves are shown: left graphs represent the displacement of the punch vs. load; right graphs represent the displacement of the lower face of the specimen vs. load (typical measurement obtained from an LVDT placed in this location).

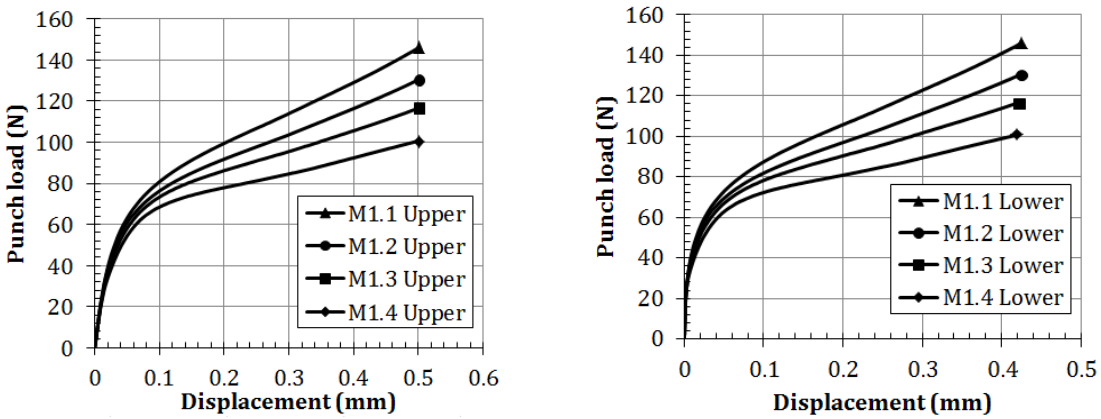

(**a**) (**b**)

Figure 3. SPT curves, (**a**) with displacement of the punch, and (**b**) with specimen lower face displacement.

The four methods currently used to obtain the elastic limit of the material via the SPT curves (Mao, Mao-projected, t/10 and CWA methods) were applied in all of the previous hypothetical materials. Two types of displacement were used: upper (the displacement of the upper face of the specimen center); and lower (the displacement of the lower face of the specimen center).

Figs. 4 and 5 show the correlation between the normalized yield loads (P_y/t^2; where t is the specimen thickness) and the yield strength σ_y of the material.

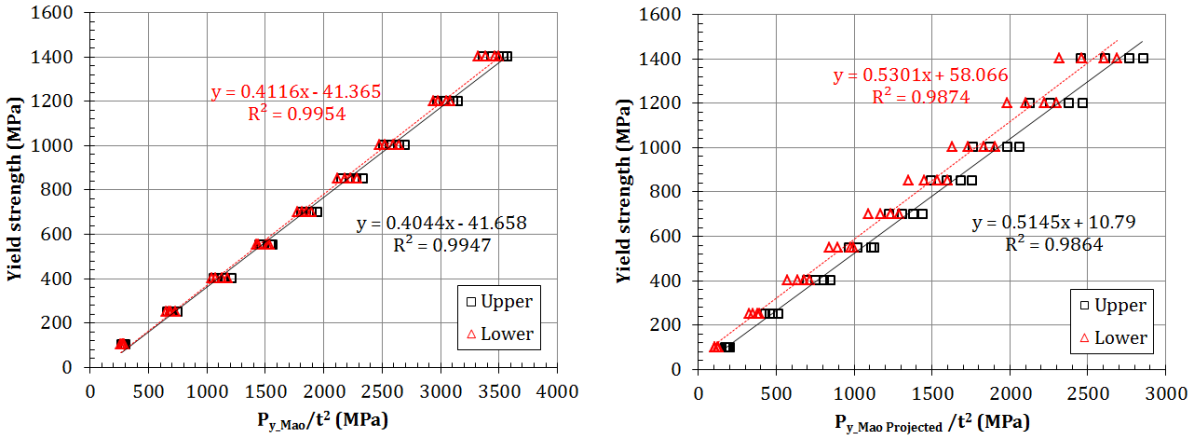

(**a**) (**b**)

Figure 4. (**a**) P_{y_Mao} correlation; (**b**) $P_{y\_MaoProjected}$ correlation.

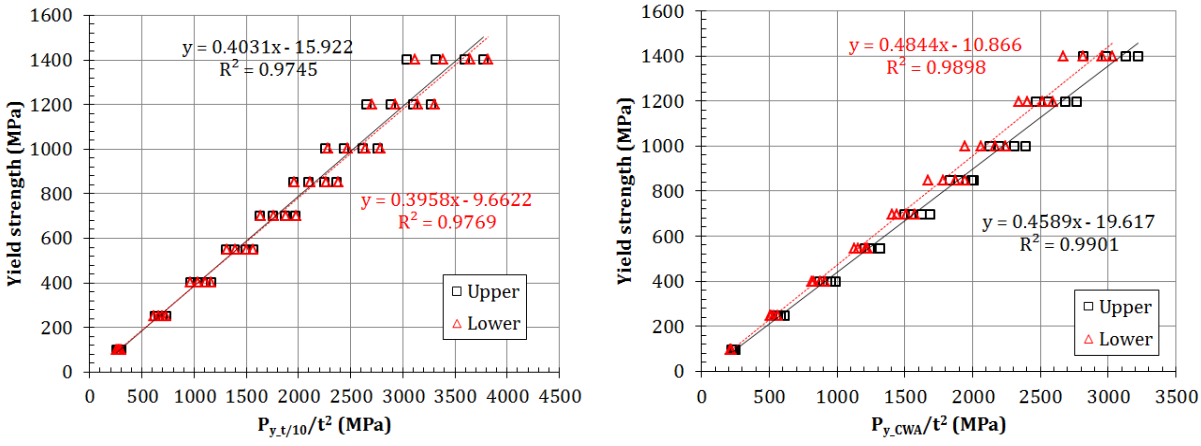

(**a**) (**b**)

Figure 5. (**a**) $P_{y\_t/10}$ correlation; (**b**) P_{y_CWA} correlation.

The SPT specimen showed a high level of plasticization in the numerical analyses for punch displacements between 0.1 mm and 0.5 mm (values used for P_y calculation in the correlation methods seen before). Thus, the hardening coefficient *n* had an important role in the behavior of the SPT specimen.

In zone I of the SPT curve, the FEM analysis showed that the beginning of the plastic zone was located just below the punch on the upper face of the sample. The yielded volume grew until reaching the lower face of the SPT specimen. This event matched with the maximum slope of the zone I of the SPT curve ($Slope_{ini}$). Thus, $Slope_{ini}$ could show a high dependence on the yield strength and low deviations due to the hardening coefficient *n*.

Fig. 6 shows the correlation between the normalized $Slope_{ini}$ ($Slope_{ini}$ /*t*; where *t* is the thickness of the specimen) and the yield strength of each material.

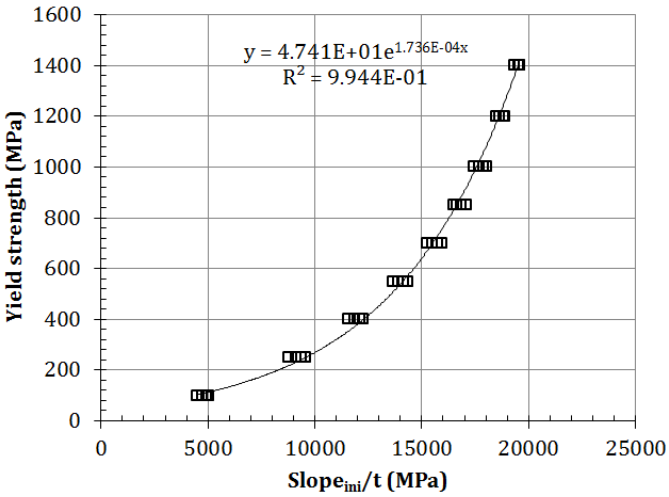

Figure 6. $Slope_{ini}$ correlation.

3.2. Experimental analyses

Six steels, DC01, DC04, HC300LA, F1110, F1140 and 15-5PH H900 were tested using standard tensile tests (ASTM E8M) and small punch tests to confirm the numerical results previously shown. Table 2 shows the mechanical properties for all tested materials, and Fig. 7 shows the SPT curves obtained from the experimental tests. The geometry and the setup of the SPT were the same as the one analyzed in the previous numerical calculations.

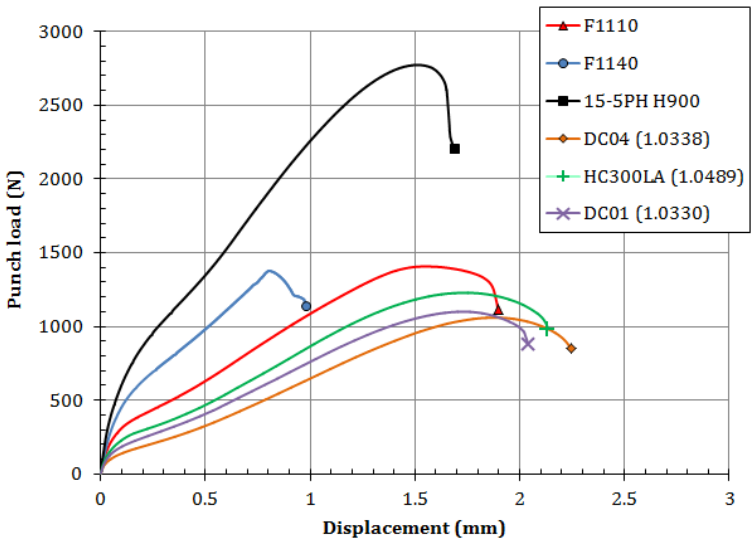

Figure 7. SPT curves of the experimental tests.

Figs. 8 to 10 show the correlation for each method with the yield strength of each alloy (obtained from the tensile tests). Fig. 11 shows the deviations between the calculated yield strengths from the experimental correlation

equations and the yield strengths obtained from the tensile tests. The most precise and reliable method was the proposed $Slope_{ini}$ method, with the CWA and t/10 methods following far behind.

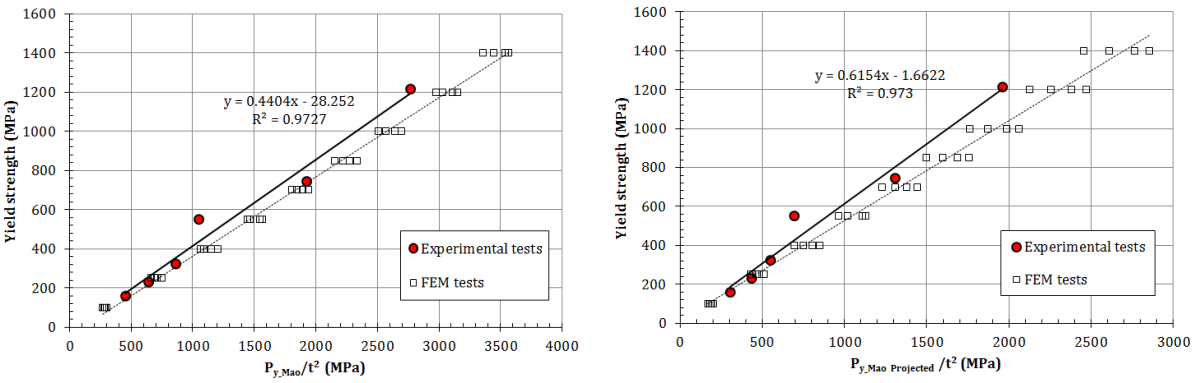

(**a**) (**b**)

Figure 8. (**a**) Mao's method correlation; (**b**) Mao Projected method correlation.

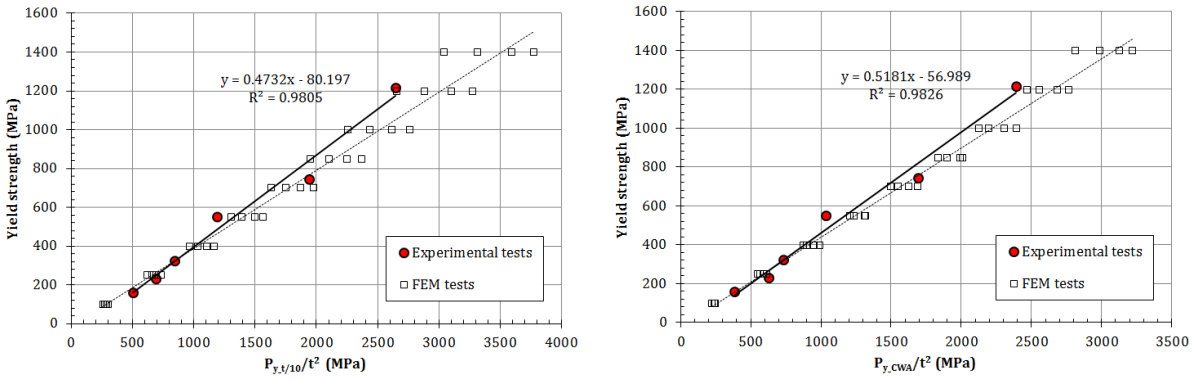

(**a**) (**b**)

Figure 9. (**a**) t/10 method correlation; (**b**) CWA method correlation.

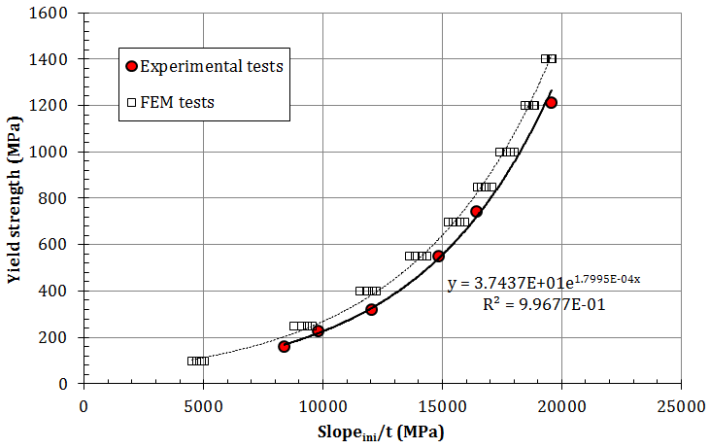

Figure 10. $Slope_{ini}$ method correlation.

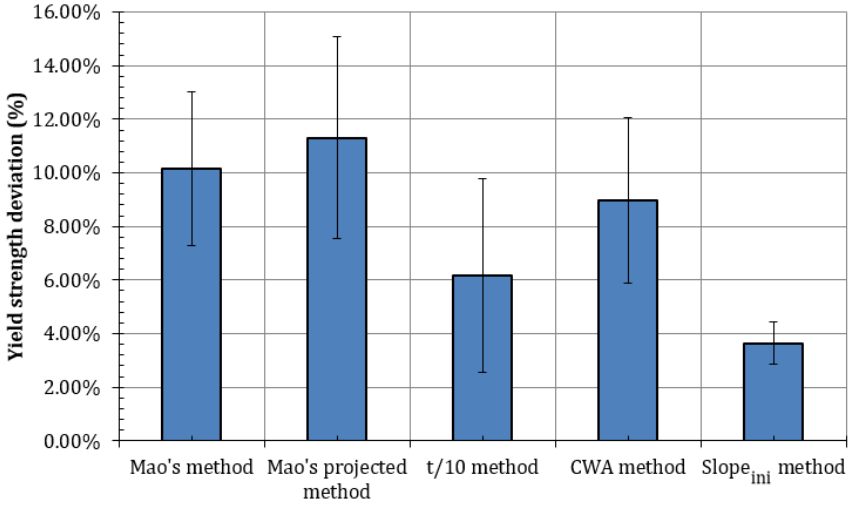

Figure 11. Deviations of the yield strength calculation.

4. Conclusions

A numerical analysis and a set of experimental tests (uniaxial tensile tests and SPTs) were performed in this research obtaining following conclusions:

a. There are two methods for measuring the displacement data for the SPT curve: the upper and the lower methods. This research demonstrated numerically that both had the same accuracy level for the yield strength correlation. The upper method is the best method for obtaining the SPT curve considering its simplicity (lower method needs the installation of an LVDT supported in the lower face of the specimen).

b. Current methods to correlate the yield strength with the SPT curve showed numerically an important dependency on the hardening coefficient *n*. Only the Mao's method showed in FEM calculations less dependency compared to the other methods, but the reason for this accuracy was based on a geometrical coincidence and not on the mechanical properties of the material. Experimental tests showed that Mao's method had a deviation level similar to the rest of the current methods. Thus, Mao's method was not more accurate than the rest of the correlation methods.

c. An improved correlation method for the yield strength σ_y was obtained using the $Slope_{ini}$ of the SPT curve. This method showed, both numerically and experimentally, a lower level of deviations and standard error compared with the current methods (Mao, Mao projected, t/10 and CWA). The "$Slope_{ini}$ method" only needs the load-displacement data from zone I and the initial part of zone II of the SPT curve to be obtained. This is much less information compared with the current methods, which need data from zones I, II and III of the SPT curve. This adds another advantage for the proposed method for materials which show brittle behavior and premature failures.

d. The "$Slope_{ini}$ method" depends on the elastic properties of the material. This investigation shows the correlation equation for steel alloys but other materials with different elastic properties should be correlated with its own correlation parameters obtained in a similar way of this research.

Acknowledgments: This research did not receive any specific grant from funding agencies in the public, commercial, or non-profit sectors.

References

1. Manahan, M.P.; Argon, A.S.; Harling, O.K. The development of a miniaturized disk bend test for the determination of postirradiation mechanical properties. *Journal of Nuclear Materials* **1981**, 103 & 104, 1545-1550, DOI: 10.1016/0022-3115(82)90820-0
2. Huang, F.H.; Hamilton, M.L.; Wire, G.L. Bend testing for miniature disks. *Nuclear Technology* **1982**, 57.2, 234-242, DOI: 10.13182/NT82-A26286
3. Lucas, G.E.; Okada, A.; Kiritani, M. Parametric Analysis of the Disc Bend Test. *Journal of Nuclear Materials* **1986**, 141-143, 532-535, DOI: 10.1016/S0022-3115(86)80096-4

4. Lucas, G.E. Review of Small Specimen Test Techniques for Irradiation Testing. *Metallurgical Transactions A* **1990**, 21A, 1105-1119, DOI: 10.1007/BF02698242
5. Calaf Chica, J.; Bravo Díez, P. M.; Preciado Calzada, M. Improved correlation for the elastic modulus prediction of metallic materials in the Small Punch Test. *International Journal of Mechanical Sciences* **2017**, 134, 112-122, DOI: 10.1016/j.ijmecsci.2017.10.006
6. Baik, J.M.; Kameda, J.; Buck, O. Development of Small Punch Tests for Ductile-brittle Transition Temperature Measurement of Temper Embrittlement Ni-Cr Steels **1986**, *ASTM STP 888*, 92-111, DOI: 10.1520/STP32997S
7. Mao, X.; Takahashi, H. Development of a further-miniaturized specimen of 3 mm diameter for tem disk small punch tests. *Journal of Nuclear Materials* **1987**, 150, 42-52, DOI: 10.1016/0022-3115(87)90092-4
8. Misawa, T.; Adachi, T.; Saito, M.; Hamaguchi, Y. Small punch tests for evaluating ductile-brittle transition behavior of irradiated ferritic steels. *Journal of Nuclear Materials* **1987**, 150, 194-202, DOI: 10.1016/0022-3115(87)90075-4
9. Mao, X.; Saito, M.; Takahashi, H. Small punch test to predict ductile fracture toughness JIc and brittle fracture toughness KIc. *Scripta Metallurgica et Materialia* **1991**, 25, 2481-2485, DOI: 10.1016/0956-716X(91)90053-4
10. Mao, X.; Takahashi, H.; Kodaira, T. Supersmall punch test to estimate fracture toughness JIc and its application to radiation embrittlement of 21/4Cr-1Mo steel. *Materials Science and Engineering A* **1992**, I50, 231-236, DOI: 10.1016/0921-5093(92)90116-i
11. CEN Workshop Agreement. *Small Punch Test Method for Metallic Materials*, CWA 15627:2007 D/E/F; CEN: Brussels, Belgium, 2007.
12. Abendroth, M.; Kuna, M. Determination of deformation and failure properties of ductile materials by means of the small punch test and neural networks. *Computational Materials Science* **2003**, 28, 633-644, DOI: 10.1016/j.commatsci.2003.08.031
13. Moreno, M.F; Bertolino, G.; Yawny, A. The significance of specimen displacement definition on the mechanical properties derived from Small Punch Test. *Materials and Design* **2016**, 95, 623-631, DOI: 10.1016/j.matdes.2016.01.148
14. Rodríguez, C.; García, J.; Cárdenas, E.; Betegón, C. Mechanical properties characterization of heat-affected zone using the small punch test. *Welding Research* **2009**, 88, 188-192.
15. Ramberg, W.; Osgood, W.R. Description of stress-strain curves by three parameters. *NACA Technical Note* **1943**, 902.